DOI 10.1007/s12182-013-0288-z

Heavy oil component characterization with multi-dimensional unilateral NMR

Liu Huabing, Xiao Lizhi*, Guo Baoxin, Zhang Zongfu, Zong Fangrong, Deng Feng, Yu Huijun, V. Anferov and S. Anferova

State Key Laboratory of Petroleum Resources and Prospecting, China University of Petroleum, Beijing 102249, China

Abstract: Heavy oil is a complicated mixture and a potential resource and has attracted much attention since the end of last century. It is important to characterize the composition of heavy oil to enhance its recovery efficiency. A designed unilateral Nuclear Magnetic Resonance (NMR) sensor with a Larmor frequency of 20 MHz and a well-defined constant gradient of 23.25 T/m was employed to acquire three-dimensional (3D) data for three heavy oil samples. The highly-constant gradient is advantageous for diffusion coefficient measurement of heavy oil. A fast data-implementation procedure including specially designed 3D pulse sequence and Inversion Laplace Transform (ILT) algorithm was adopted to process the data and extract 3D T_1-D-T_2 probability function. It indicates that NMR relaxometry and diffusometry are useful to characterize the components of heavy oil samples. NMR results were compared with independent measurements of fractionation and gas chromatography analysis.

Key words: Heavy oil, multi-dimensional NMR, unilateral sensor

1 Introduction

Heavy oil has high viscosity and density (API gravity in the range of 10°-20°, viscosity between 100 and 10,000 cp). The heavy oil reserves in the world are about 6 trillion barrels in situ (Galford and Marschall, 2000). With the continuous decline of conventional oil reservoirs, the commercial potential of heavy oil has attracted great attention. However, its high viscosity restricts heavy oil production flows. The major method applied in oil fields is to inject steam into the heavy oil reservoirs to reduce its viscosity, which needs careful manipulation due to the complex properties of heavy oil (Mullins et al, 2007; Zheng and Hirasaki, 2008; Hirasaki et al, 2002). Therefore, it is critical to know more about the components of heavy oil so as to optimize the recovery, upgrading, refining and transportation procedures (Mullins, 2005; Latorraca et al, 1998; Pena and Hirasaki, 2003).

A number of analytical techniques have been used to provide information about the components of complex fluids. These include gas chromatography, optical and NMR spectroscopy. In the context of this article, gas chromatography cannot detect the complete components of heavy oils because large molecules with more than 36 carbon atoms are difficult to transfer into the gas phase. However, those large molecules hold dominant ratios in heavy oil samples. Optical spectroscopy is unsuitable as heavy oils are largely opaque. NMR spectroscopy becomes inefficient due to the overlap of spectra from individual molecules. Compared to that, NMR relaxometry and diffusometry are robust enough to detect complete components of heavy oil because of the relationship between chain length and dynamic characteristics (T_1, T_2, and D) of its molecules (Freed et al, 2005; Freed, 2007).

A high-enough magnetic field gradient should be applied to encode slow diffusion characterization of heavy oil. In this paper, a designed NMR unilateral sensor with a highly-constant magnetic field gradient of 23.25 T/m was used to provide information about the complicated components of heavy oil. A multi-dimensional NMR technique and a fast data-implementation procedure were developed to measure, process and analyze components of heavy oil samples. 3D NMR distribution and 2D projection of oil samples were presented and discussed.

2 Spin-dynamics of heavy oils

Spin dynamics of a fluid are characterized by the longitudinal relaxation time T_1, transverse relaxation time T_2 of spin system and diffusion coefficient D of the entire molecule (Blümich, 2005; Dunn et al, 2002; Wong, 1999; Cowan, 1997). In a complicated hydrocarbon mixture, small molecules generally diffuse faster than large ones. Thus, the diffusion coefficient of a specific hydrocarbon molecule is related to its size, or chain length. The integral fluid environment influences molecular diffusion as well (Lisitza et al, 2009). The general scaling relationship between diffusion

*Corresponding author. email: xiaolizhi@cup.edu.cn
Received October 22, 2012

coefficients and molecular length in oils is (Freed and Hürlimann, 2010)

$$D_i = A \cdot \bar{N}^{-\beta} \cdot N_i^{-\nu} \quad (1)$$

where D_i and N_i are the self-diffusion coefficient and chain length of the i-th hydrocarbon molecule, A is a factor independent of composition, the mean chain length $\bar{N}$ and its index β determine the overall environment surrounding the hydrocarbon molecules, exponent ν reflects the equilibrium configurations of oil chains.

Relaxation is typically dominated by intra-molecular nuclear dipole interactions which are modulated by molecular motion (Blümich, 2005). Longitudinal relaxation time T_1 characterizes the energy exchange rate between the spin system and the lattice or the environment of a nucleus with surrounding molecules, while transverse relaxation time T_2 describes the dipole-dipole interaction in the spin system. As Fig. 1 shows, for molecules at the fast motion limit ($\omega_L\tau_C<1$, ω_L is Larmor frequency of nuclei, here we use 20 MHz, τ_C is the correlation time of molecular reorientation), T_1 and T_2 relaxation measurements provide identical results, both decrease as τ_C increases; for molecule in slow motion limit, T_1 is generally larger than T_2 with descending motion speed, which may result from the intra-molecular aggregation and super-molecular formation (Lisitza et al, 2009). The longer the reorientation times for molecule, the larger the T_1-T_2 contrast. As a result, components with small relaxation difference show light oil properties, and a large T_1/T_2 ratio proves the existence of large molecules in the NMR measurements of large molecules in the NMR measurements of heavy oils.

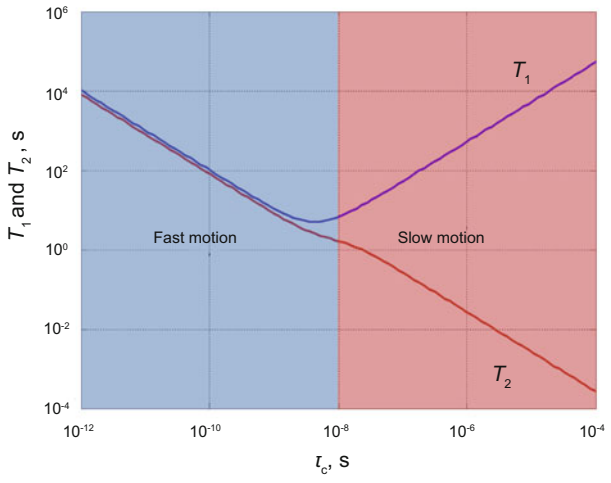

Fig. 1 NMR relaxation dynamics of molecules at a Larmor frequency of 20 MHz

Similar to diffusion coefficients, relaxation times are also related to the molecular chain length and the overall environment at the fast motion limit. The relationship is simplified as (Freed and Hürlimann, 2010)

$$T_{1i} = T_{2i} = B \cdot \bar{N}^{-\gamma} \cdot N_i^{-\kappa} \quad (2)$$

where B is the proportional factor independent of chain length, friction and internal viscosity, γ and κ are empirical exponents in this power law and are fitted from the experiments with n-alkanes.

3 Hardware

A special NMR unilateral sensor with a well-defined high magnetic field gradient was designed by our group. The designed probe is shown in Fig. 2(a). The sensor consisted of a magnet system and a radio frequency (RF) system.

The U-shape magnet system (Anferova et al, 2002; 2004) contained two permanent (NdFeB) magnet blocks separated by a small gap of 17 mm and positioned on an iron yoke. The dimensions of the permanent magnets were 40×40×100 mm^3. Since the direction of magnetic polarization was along y axis and magnets were placed face to face with anti-parallel magnetization, the magnetic field flux density was mostly parallel to the surface of magnets. The corresponding ^1H NMR frequency was 20 MHz.

The RF system contains a four-turn oval surface coil. The coil is made of copper wire with a diameter of 0.6 mm and embedded in a position 6 mm above the surface of magnets. The purpose of this elevation is to improve the homogeneity of the magnetic field on the surface of the RF coil. Two capacitors in a shielded box are used to tune and match the impedance and frequency of the RF circuit.

Simulation of the sensitive volume of the sensor is shown in Fig. 2(b). The thickness of the nearly flat sensitive sheet is approximately 0.3 mm at a distance of y=6.5 mm above the magnet surface. The gradient of the magnetic field in this range is calculated to be G_0 =23.25 T/m.

Three pure liquids, distilled water, ethanol and acetone, with known diffusion coefficients (2.30×10^{-9} m^2/s, 1.05×10^{-9} m^2/s and 5.69×10^{-9} m^2/s at 25 °C) are used to calibrate the magnetic field gradient of the unilateral sensor from a mono-exponential fit of a series of spin echoes with different echo intervals τ. According to spin echo attenuation law $\ln(Amp/Amp_0) = -(2D\gamma^2\tau^3/3)\cdot G_0^2$ (Bloch, 1946; Torrey, 1956), nearly linear fitting lines with a slope of $-G_0^2$ are found in Fig. 2(c). The calibrated gradient of the unilateral sensor corresponds very well to the calculated value.

4 Methodology

4.1 3D Pulse sequence

The designed pulse sequence shown in Fig. 3 contained three distinct sections. Section I was T_1 encoding part. A series of 90° pulses were applied to eliminate magnetization along the longitudinal axis. t_S was the saturation delay time which varied between eight pulses as t_S/n. After recovery time τ_1, a subsequent 90° pulse was used to tip the saturated magnetization on the transverse plane. Section II was D encoding part with the logarithmically increased diffusion editing time τ_2. A 180° pulse was applied to refocus the dephasing transverse magnetization and the direct echo was

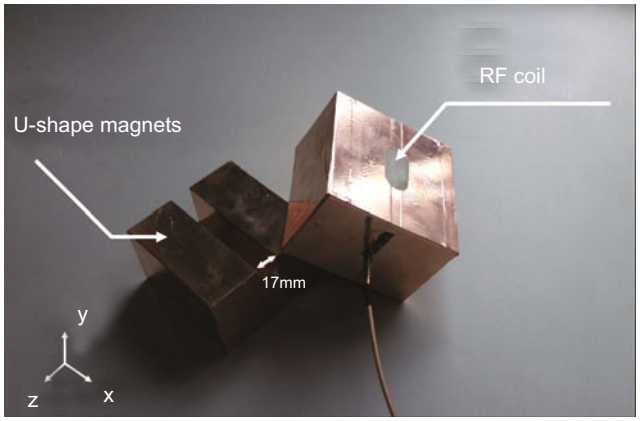

(a)

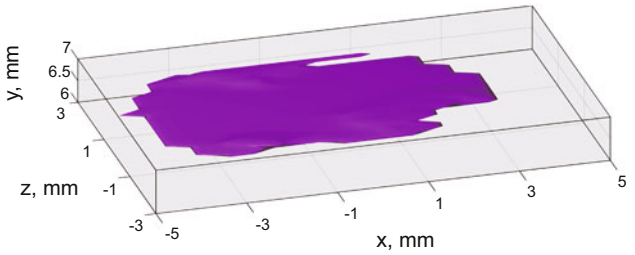

(b)

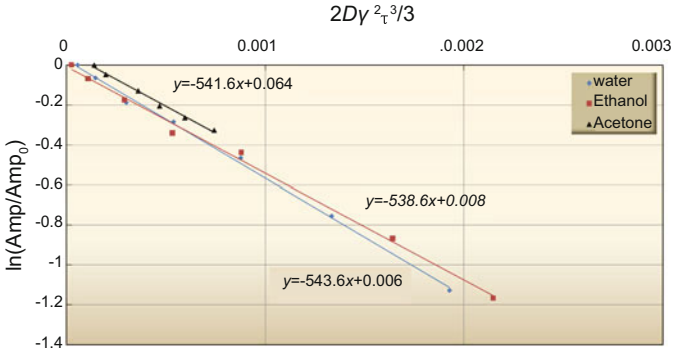

(c)

Fig. 2 (a) Designed unilateral sensor. (b) Simulation of the sensitive volume of designed sensor. The sensitive volume of the sensor is a thin sheet. (c) Gradient calibration results. Linear fitting lines of different liquids are fitted as a factor of $-G_0^2$. The results showed a good agreement with the simulated gradient result of 23.25 T/m

received to edit diffusion coefficients. Section III was a regular CPMG pulse sequence for $T_{2\text{eff}}$ encoding. The echo number was constant and t_E was a sufficiently short echo spacing to minimize the diffusion influence.

4.2 3D ILT algorithm

In this paper, a fast 3D Inversion Laplace Transform (ILT) algorithm was developed based on the designed pulse sequences. The measured magnetization M (τ_1, τ_2, nt_E) can be written as

$$M(\tau_1, \tau_2, nt_E) = \sum\sum\sum k_{T_1}(T_1, \tau_1) k_D(D, \tau_2) k_{T_{2\text{eff}}}(T_{2\text{eff}}, nt_E) F(T_1, D, T_{2\text{eff}}) \quad (3)$$

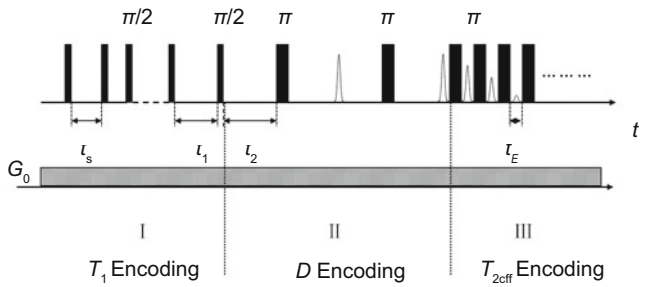

Fig. 3 A designed pulse sequence used in the multi-dimensional NMR experiments for heavy oil

where

$$k_{T_1}(T_1, \tau_1) = 1 - \exp(-\frac{\tau_1}{T_1}),$$
$$k_D(D, \tau_2) = \exp\left[-\frac{4}{3} D(\gamma G_0)^2 \tau_2^3\right] \exp(-\frac{2\tau_2}{T_{2\text{eff}}}), \quad (4)$$
$$k_{T_{2\text{eff}}}(T_{2\text{eff}}, nt_E) = \exp(-\frac{nt_E}{T_{2\text{eff}}})$$

where, γ is the gyromagnetic ratio and G_0 is the constant gradient provided by the unilateral NMR sensor, F (T_1, D, $T_{2\text{eff}}$) is the joint probability density function of interest, and kernels K_{T1}, K_D, and $K_{T2\text{eff}}$ are exponential factors related to respective NMR quantities.

To invert 3D NMR data, scientists prefer to compress these three kernel matrices separately (Arns et al, 2007) or cast them to be an ensemble (Sun and Dunn, 2005). In this work, we coupled K_{T1} and K_D to be a new one K_C using tensor products because of the comparable size:

$$K_C = K_{T_1} \otimes K_D \quad (5)$$

The measured magnetization becomes

$$M = K_C F K_{T_{2\text{eff}}} \quad (6)$$

Through this procedure, the 3D inversion transformation was simplified to a 2D problem which has been solved effectively (Venkataramanan et al, 2002; Song, 2009; Hürlimann et al, 2002; Liu et al, 2013). Here, we would like to give an explicit introduction of this 2D solving method. As an ill-posed problem, Tikhonov regularization was employed to minimize the cost function:

$$\hat{F} = \arg\min_{F \geq 0} \left\| M - K_C F K_{T_{2\text{eff}}} \right\|^2 + \alpha \left\| F \right\|^2 \quad (7)$$

where α is the regularization factor related to the signal-to-noise ratio of data, and $\|\cdot\|$ represents the Frobenius norm of a matrix.

To accelerate the inversion procedure, data compression is implemented with a singular value decomposition method before solving Eq. (7). Let

$$K_C = U_1 \cdot \sum_1 \cdot V_1^{'}$$
$$K_{T_{2\text{eff}}} = U_2 \cdot \sum_2 \cdot V_2^{'} \quad (8)$$

The compressed magnetization $\tilde{M} = U_1^{'} M U_2$, and $\tilde{K}_C = \sum_1 \cdot V_1^{'}, \tilde{K}_{T_{2\text{eff}}} = \sum_2 \cdot V_2^{'}$.

To facilitate the inversion procedure, the constraints solution is solved in one-dimensional space:

$$f_r = \tilde{K}_0^{'}(\tilde{K}_0 \cdot \tilde{K}_0^{'} + \alpha \cdot I)^{-1} \tilde{m}_r \quad (9)$$

where $\tilde{K}_0 = \tilde{K}_C \otimes \tilde{K}_{T_{2\text{eff}}}$. 3D probability distribution function F is obtained from realigning the solved f_r.

This 3D inversion procedure was implemented on a 2.8 GHz PC with 4 GB of memory. In 3D experiments with a SNR of 10-20, the inversion result (50×50×50 data points) was obtained in 10 seconds with the optimal smoothing parameter α. The performance of the 3D inversion algorithm is demonstrated in rock experiments.

5 Experimental results

In an inhomogeneous field, the information extracted from echoes decay is not T_2 but $T_{2\text{eff}}$, which is a weighted sum of longitudinal and transverse relaxation rates (Hürlimann and Griffin, 2000):

$$\frac{1}{T_{2\text{eff}}} = \frac{1}{T_2} - n_z^2 \left(\frac{1}{T_2} - \frac{1}{T_1} \right) \quad (10)$$

where n_z^2 was a normalized integral factor quantifying the inhomogeneity of the static magnetic and RF fields of the sensor.

Distilled water, ethanol and acetone were used to calibrate n_z^2 so as to correctly measure $T_{2\text{eff}}$ to T_2. Firstly, the mean values of the longitudinal relaxation time T_1 and transverse relaxation time T_2 of pure liquids were measured in a homogenous magnetic field at a comparable frequency of 23 MHz (Micro-MR, NIUMAG). Secondly, the mean value of the effective relaxation time $T_{2\text{eff}}$ of the relevant liquid was measured using the unilateral sensor. According to Eq.(10), the factor n_z^2 of this sensor was estimated approximately as 0.13, which is slightly different from the values reported elsewhere (Hürlimann and Griffin, 2000; Chelcea et al, 2009; Goelman and Prammer, 1995).

Three heavy oil samples were measured using the described pulse sequence and 3D ILT algorithm was implemented to process data. T_1 editing time τ_1 varied in 20 steps logarithmically from 0.5 ms to 6000 ms. Diffusion coefficients editing time τ_2 varied in 10 steps logarithmically from 0.1 ms to 3 ms. The echo interval t_E was 0.12 ms. Results are presented in Fig. 4. Two reference planes were marked to clearly observe the extension of NMR properties in heavy oil. The vertical plane was a plane of T_1=T_2 and the transverse plane corresponded to the limit of diffusion coefficients value of heavy oil, 10^{-12} m^2/s. Additionally, these three heavy oil samples with increasing viscosity from sample 1 to sample 3 were fractionated and analyzed by gas chromatography.

3D NMR distribution maps of heavy oil samples are presented in the first column of Fig. 4, and display more complicated behavior with increasing viscosity. Two entities were observed in the 3D map of oil sample 1 at a diffusion coefficient around 10^{-11} m^2/s. For sample 2, there appeared three entities which were located near diffusion coefficients of 10^{-11} m^2/s and 10^{-9} m^2/s. Four entities were observed in 3D map of oil sample 3 with the highest viscosity. These entities can be divided into two groups with diffusion coefficient values around 10^{-11} m^2/s and 10^{-9} m^2/s, respectively. The main entities were observed at a diffusion coefficient value of 10^{-11} m^2/s, and with a larger longitudinal relaxation time T_1 than transversal relaxation time T_2 in all 3D maps, indicating the existence of large molecules with long chain lengths. Some unique molecular substances, like asphaltene, result in the complexity of heavy oil. The other entities corresponding to diffusion coefficients of 10^{-9}-10^{-10} m^2/s had nearly equal relaxation time, and were designated as light components. Sample 3 had the strongest signal at this diffusion coefficient range, indicating the highest level of light components. The fractionation analysis also confirmed that sample 3 contained a ratio of alkane components of almost 50 wt%, compared to 40.8 wt% of sample 1 and 43.6 wt% of sample 2.

From projected T_1-T_2 correlation maps (column 2 of Fig. 4) it is obvious that T_1 was bigger than T_2 for all samples, and T_1/T_2 ratio risen up with an increase of viscosity. This dependence of T_1/T_2 ratio with viscosity can be explained as slow motion because of the existence of large, even super-large molecules according to Fig.1. These large and super-large molecules can easily aggregate to large structures, subsequently entangle small molecules like alkane leading to relaxation contrast. Fractionation analysis showed that the ratio of asphaltene is 7 wt% in sample 1, 10.5 wt% in sample 2 and 15 wt% in sample 3, in good accordance with the conclusions obtained from projected T_1-T_2 correlation maps.

In T_2-D maps of samples 1, 2 and 3 (column 3 of Fig. 4), peaks with the highest intensity were located in the diffusion coefficient range of 10^{-10}-10^{-12} m^2/s. These peaks became broader along diffusion coefficient axis with increasing viscosity of the oil samples, indicating the complexity of chemical components. For sample 3, the diffusion coefficients was 10^{-12} m^2/s, indicating that the molecules of sample 3 were different in size and more complex compared to those of sample 1.

Compared to T_2-D correlation distribution, a peak-shift appeared along T_1 dimension in T_1-D correlation distribution. Signals corresponding to a diffusion coefficient range of 10^{-9} -10^{-10} m^2/s shifted much less than the signals corresponding to 10^{-10}-10^{-12} m^2/s, implying these components with diffusion coefficient range of 10^{-9}-10^{-10} m^2/s are light ones with short molecular chain lengths. An exceptional signal with a relaxation time of 10^{-3} s had no shift along T_1 dimension in sample 3, and it might be attributed to groups of small molecules entangled inside the aggregated large structures.

Independent gas chromatography analysis was performed on an Agilent 7890A chromatograph. Nitrogen with a concentration of 99.999% was used as carrier gas with an HP-1 elastic quartz capillary column (60m×0.25mm×0.25mm). The initial system temperature of 40 °C was kept for 10 min, and then increased to 70 °C at a rate of 4 °C/min, continue to 300 °C at a rate of 8 °C/min.

Two main populations were found along the carbon number axis in gas chromatography results of these three

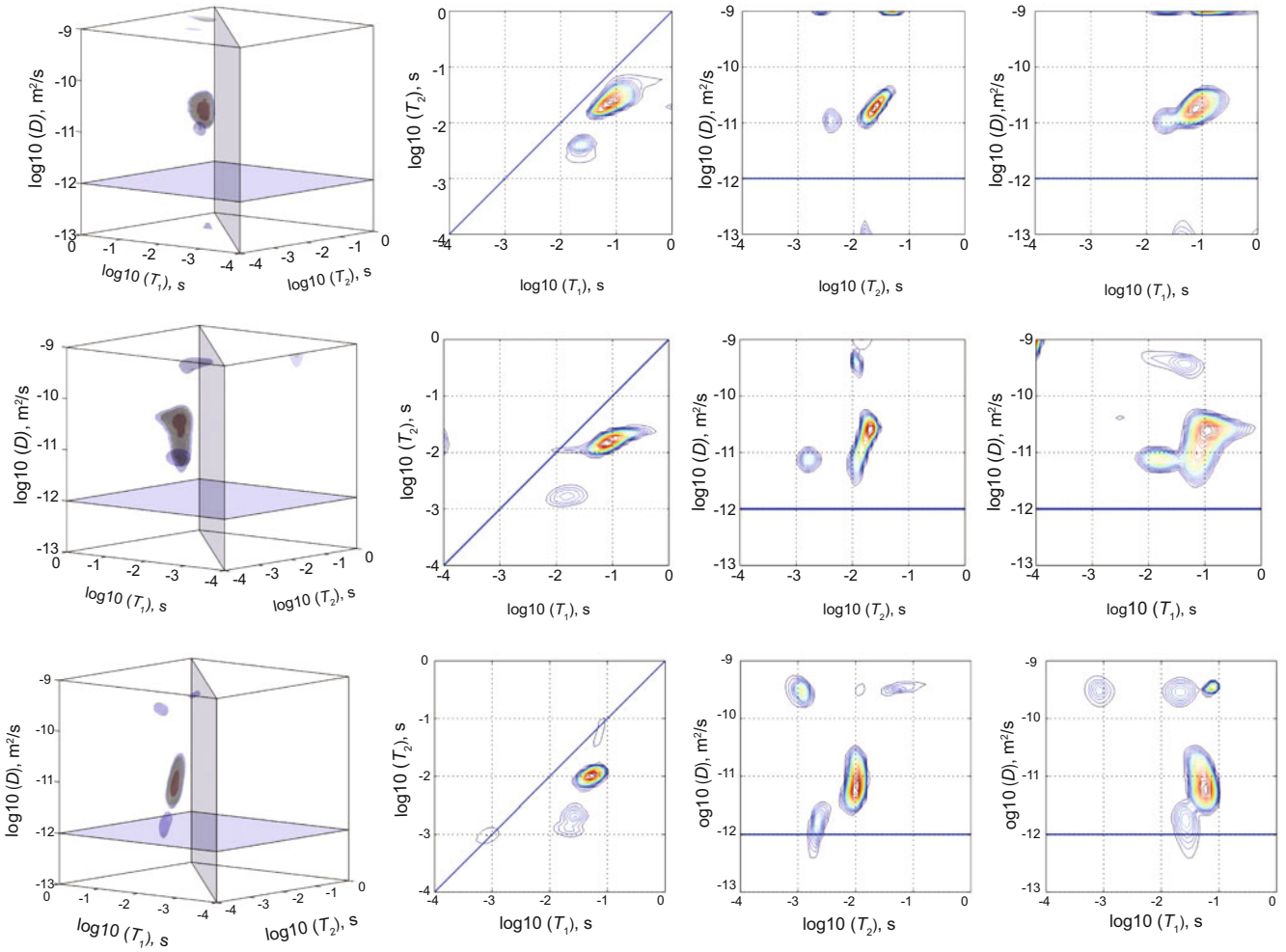

Fig. 4 Multi-dimensional NMR distributions of heavy oil, a) sample 1, b) sample 2, c) sample 3. Viscosity increased from top to bottom. T_{2eff} was converted to T_2 according to the factor calibrated by pure liquid

heavy oil samples (Fig. 5). Because of the limitation of transforming molecules with carbon number larger than 36 to gas phase, gas chromatography is a partial measurement in components analysis of heavy oils. The measured carbon chain length of molecules extends widely from C_9 to C_{36}, corresponding to the diffusion coefficients of 10^{-9}-10^{-11} m^2/s according to Eq.(1). These components are explained to be light- and moderate-components in heavy oils. In the measured carbon number spectrum of sample 1 and 2 (black and red curves in Fig. 5), the mean values of the distribution are obviously smaller than the value of sample 3 (green curve in Fig. 5), which corresponds to higher diffusion coefficients in the NMR signal distribution of sample 1 and 2. The similarity of measured carbon number distributions in samples 1 and 2 relates to the similar pattern of 3D T_1-D-T_2 distributions in the range of diffusion coefficients from 10^{-9} m^2/s to10^{-11} m^2/s. For sample 3, there still exists a large amount of signals with the relaxation time of 10^{-3} -10^{-2} s and diffusion coefficients of 10^{-11} -10^{-12} m^2/s, suggesting the heavy components bearing large molecules with carbon numbers above 36. Consequently, a full characterization of components information in the three heavy oil samples can be extracted from 3D NMR relaxometry-diffusometry measurements, compared to the gas chromatography analysis.

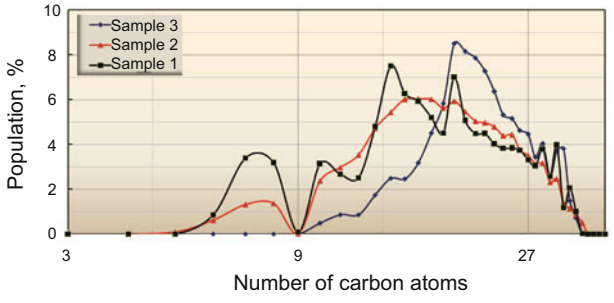

Fig. 5 Gas chromatography results of samples 1, 2 and 3. The population distribution is plotted on a logarithmical scale because of the exponential relationship between carbon chain length and spin dynamical properties given in Eqs.(1) and (2)

6 Conclusion

The designed unilateral NMR sensor with simple construction and constant high gradient (G_0=23.25 T/m) and a fast 3D data-implementation including designed pulse sequence and ILT algorithm are successfully applied in the analysis of heavy oil samples. The final results show more capabilities of using NMR relaxometry and diffusometry to

characterize the heavy oils components.

Among these three samples, NMR signals with diffusion coefficients of 10^{-9}-10^{-11} m^2/s corresponds to the light- and moderate components in heavy oils, and signals with relaxation time of 10^{-3}-10^{-2} s and diffusion coefficients of 10^{-11} -10^{-12} m^2/s are explained to be heavy components in heavy oils. Although the later signals have totally out of the valid range in gas chromatography, they can still be easily detected in 3D NMR relaxometry and diffusometry distribution and confirmed by fractionation analysis.

Acknowledgements

The authors gratefully thank financial supports from the National Science Foundation of China (Grant No. 41074102 and 41130417), "111 Program, Supported by the Programme of Introducing Talents of Discipline to Universities" (B13010) and Program for Changjiang Scholars and Innovative Research Team in University.

References

Anferova S, Anferov V, Adams M, et al. Construction of the NMR-MOUSE with short dead time. Concepts in Magnetic Resonance. 2002. 15(1): 15-22

Anferova S, Anferov V, Rata D G, et al. A mobile NMR Device for measurements of Porosity and Pore size Distributions of Drilled core Samples. Magnetic Resonance Engineering. 2004. 23B: 26-32

Arns C H, Washburn K E and Callaghan P T. Multidimensional NMR Inverse Laplace Spectroscopy in Petrophysics. Petrophysics. 2007. 48(5): 380-392

Bloch F. Nuclear induction. Physical Review. 1946. 70(7): 460-474

Blümich B. Essential NMR. Springer. 2005

Chelcea R L, Fechete R, Culea E et al. Distribution of transverse relaxation times for soft-solids measured in strongly inhomogeneous magnetic fields. Journal of Magnetic Resonance. 2009. 196: 178-190

Cowan B. Nuclear Magnetic Resonance and Relaxation. Cambridge: Cambridge University Press. 1997

Dunn K J, Bergman D J and Latorraca G A. Nuclear Magnetic Resonance: Petrophysical and Logging Applications. Pergamon: Elsevier Science. 2002

Freed D E and Hürlimann M D. One-and two-dimensional spin correlation of complex fluids and the relation to fluid composition. Comptes Rendus Physique. 2010. 11: 181-191

Freed D E, Burcaw L and Song Y Q. Scaling laws for diffusion coefficients in mixtures of alkanes. Physics Review Letters. 2005. 94(6): 067602

Freed D E. Dependence on chain length of NMR relaxation times in mixtures of alkanes. The Journal of Chemical Physics. 2007. 126 (17): 174502

Goelman G and Prammer M G. The CPMG pulse sequence in strong magnetic field gradients with applications to oil-well logging. Journal of Magnetic Resonance. 1995. 113: 11-18

Hirasaki G J, Lo S W and Zhang Y. NMR properties of petroleum reservoir fluids. Magnetic Resonance Imaging. 2002. 21: 269-277

Hürlimann M D, Venkataramanan L and Flaum C. The diffusion-spin relaxation time distribution function as an experimental probe to characterize fluid mixtures in porous media. Journal of Chemical Physics. 2002. 117(22): 10223-10232

Hürlimann M D and Griffin D D. Spin dynamics of Carr-Purcell-Meiboom-Gill-like sequences in grossly inhomogeneous B_0 and B_1 fields and application to NMR well logging. Journal of Magnetic Resonance. 2000. 143: 120-135

Latorraca G A, Dunn K J, Webber P R, et al. Low-field NMR determinations of the properties of heavy oils and water-in-oil emulsions. Magnetic Resonance Imaging. 1998. 16: 659-662

Lisitza N V, Freed D E, Sen P N, et al. Study of Asphaltene Nanoaggregation by Nuclear Magnetic Resonance. Energy & Fuels. 2009. 23: 1189-1193

Liu H B, Xiao L Z, Yu H J, et al. Probing Structural Compositions of Porous Media with 2D-NMR. Applied Magnetic Resonance. 2013. 44: 543-552

Mullins O C, Sheu E Y, Hammami A, et al. Asphaltenes, Heavy oils, and Petroleomics. Springer. 2007

Mullins O C. Review of the molecular structure and aggregation of asphaltenes and petroleomics. Society of Petroleum Engineers. 2005. Paper: SPE 95801

Galford J E and Marschall D M. Combing NMR and conventional logs to determine fluid volumes and oil viscosity in heavy-oil resercoirs. Paper SPE 63257 presented at Dallas, 1-4 October 2000, Dallas, USA

Pena A A and Hirasaki G J. Enhanced characterization of oilfield emulsions via NMR diffusion and transverse relaxation experiments. Advances in Colloid and Interface Science. 2003. 105: 103-150

Song Y Q. A 2D NMR method to characterize granular structure of dairy products. Progress in Nuclear Magnetic Resonance Spectroscopy. 2009. 55: 324-334

Sun B Q and Dunn K J. A global inversion method for multi-dimensional NMR logging. Journal of Magnetic Resonance. 2005. 172: 152-160

Torrey H C. Bloch equations with diffusion terms. Physical Review. 1956. 104(3): 563-565

Venkataramanan L, Song Y Q and Hürlimann M D. Solving Fredholm integrals of the first kind with tensor product structure in 2 and 2.5 dimensions. IEEE Transactions on Signal Processing. 2002. 50(5): 1017-1026

Wong P Z. Methods in the Physics of Porous Media. London: Academic Press. 1999

Xiao L Z, Liu H B, Zhang Z F, et al. Probing Internal Gradients Dependence in Sandstone with Three-dimensional NMR Experiment. Microporous & Mesoporous Materials (in Press)

Zheng Y and Hirasaki G J. NMR measurement of bitumen at different temperatures. Journal of Magnetic Resonance. 2008. 192: 280-293

(Edited by Zhu Xiuqin)